

Transformers for dynamical systems learn transfer operators in-context

Anthony Bao,^{1,*} Jeffrey Lai,^{2,*} and William Gilpin^{3,†}

¹*Department of Electrical & Computer Engineering,
The University of Texas at Austin, Austin, Texas 78712, USA*

²*The Oden Institute, The University of Texas at Austin, Austin, Texas 78712, USA*

³*Department of Physics, The University of Texas at Austin, Austin, Texas 78712, USA*

(Dated: February 24, 2026)

Large-scale foundation models for scientific machine learning adapt to physical settings unseen during training, such as zero-shot transfer between turbulent scales. This phenomenon, in-context learning, challenges conventional understanding of learning and adaptation in physical systems. Here, we study in-context learning of dynamical systems in a minimal setting: we train a small two-layer, single-head transformer to forecast one dynamical system, and then evaluate its ability to forecast a *different* dynamical system without retraining. We discover an early tradeoff in training between in-distribution and out-of-distribution performance, which manifests as a secondary double descent phenomenon. We discover that attention models apply a transfer-operator forecasting strategy in-context. They (1) lift low-dimensional time series using delay embedding, to detect the system’s higher-dimensional dynamical manifold, and (2) identify and forecast long-lived invariant sets that characterize the global flow on this manifold. Our results clarify the mechanism enabling large pretrained models to forecast unseen physical systems at test without retraining, and they illustrate the unique ability of attention-based models to leverage global attractor information in service of short-term forecasts.

Scientific foundation models are pretrained on vast amounts of data, with a goal of discovering generalizable patterns applicable to unseen problem domains. Animating such efforts is the observation that, at sufficient scale, these models exhibit the emergent capability to solve unseen tasks during testing [1]. For example, models trained on low-resolution turbulent snapshots exhibit the spontaneous ability to forecast higher-resolution grids [2–4]. In some cases, models trained on certain classes of PDEs, like diffusion equations, develop the ability to forecast new classes of PDEs, like wave equations [5]. These findings align with similar observations for large language models, which exhibit the emergent ability to solve unseen tasks, like novel logical puzzles or mathematical derivations, at sufficient scale [6].

The underlying mechanism, in-context learning, differs from classical machine learning approaches that dichotomize learning during training from testing during inference. Instead, pretraining provides a sufficiently large model with vast background experience and an underlying world model, allowing it to quickly adapt to new tasks based on minimal context [7, 8]. In traditional scientific machine learning, a trained model acts as a surrogate for the dynamical process that generated the training data, and so a trained model can, at best, only generate test outputs matching the distribution of the training data, known as *in-distribution (ID) generalization*. In contrast, in-context learning enables *out-of-distribution (OOD) generalization* on new data distributions [9]. However, the underlying mechanisms enabling in-context learning and OOD generalization in SciML are

poorly understood, even as recent empirical studies have uncovered robust signatures of generalization in areas as diverse as turbulence closure modelling, large eddy convection, or magnetohydrodynamics [10, 11].

To clarify the origin of in-context learning in scientific machine learning, we draw inspiration from recent works that train minimal language models, in order to probe the mechanistic origin of in-context learning [12–14]. We train a small transformer model on a univariate trajectory originating from a single dynamical system (denoted Train-ID), and we then evaluate its ability to both (1) forecast a different trajectory from the *same* dynamical system (Test-ID), and (2) forecast a trajectory from a *different* dynamical system (Test-OOD). We first generate a trajectory $\mathbf{y}(t) \in \mathbb{R}^D$ from the D -dimensional ordinary differential equation $\dot{\mathbf{y}} = \mathbf{f}(\mathbf{y})$, $\mathbf{y}(0) = \mathbf{y}_0^{\text{train}}$. Train-ID consists of a univariate training time series x_1, x_2, \dots, x_T representing evenly-spaced samples of the first coordinate of the full trajectory $\mathbf{y}(t)$. In order to use language modeling approaches, we convert these continuous values to discrete tokens by uniformly quantizing them into V evenly-spaced bins (token IDs). This same approach is used by leading foundation models for zero-shot time series forecasting [15]. For simplicity, hereafter we use x_t to refer to elements of the tokenized univariate time series.

A probabilistic forecast model $\hat{p}(x_{t+1}|\mathbf{x}_C) \in \mathbb{R}^V$ accepts the context vector $\mathbf{x}_C \in \mathbb{Z}^C$ comprising C past tokens, and returns a vector $\hat{p}(x_{t+1}) \in \mathbb{R}^V$ corresponding to next-token probabilities across the vocabulary. Following prior works on minimal transformers, we model \hat{p} using a minimal GPT-like transformer, comprising two layers with a single attention head each, and relative positional encoding [6] (Appendix B). For each input context \mathbf{x}_C , transformers compute self-attention, comprising C^2 pairwise comparisons among all tokens in the context, re-

* These authors contributed equally to this work.

† wgilpin@utexas.edu

sulting in attention weights $A(\mathbf{x}_C) \in \mathbb{R}^{C \times C}$ that quantify the relative importance of each past token in influencing the next-token probabilities.

We train the transformer $\hat{p}(x_{t+1}|\mathbf{x}_C)$ on Train-ID using standard gradient-based optimization with cross-entropy loss, which aligns $\hat{p}(x_{t+1}|\mathbf{x}_C) \in \mathbb{R}^V$ with the empirical next-token distribution $p(x_{t+1}|\mathbf{x}_C)$ in the training data. After training, multistep forecasts are generated by sampling tokens from the transformer $\hat{x}_{t+1} \sim \hat{p}(x_{t+1}|\mathbf{x}_C)$ and appending each sample to the context autoregressively. Throughout training, we measure the transformer’s ability to forecast an unseen trajectory from the same dynamical system (Test-ID) denoted $\hat{\mathbf{y}} = \mathbf{f}(\mathbf{y})$, $\mathbf{y}(0) = \mathbf{y}_0^{\text{test}}$ as well as its ability to forecast a trajectory from an unseen system (Test-OOD) denoted $\hat{\mathbf{y}} = \mathbf{g}(\mathbf{y})$, $\mathbf{y}(0) = \mathbf{y}_0$. We repeat all experiments by training new transformers on each of 100 different pairs of systems drawn from a large database of ordinary differential equations [16], allowing measurement across a variety of distinct physical systems.

Remarkably, we observe that, in this minimal setting, small pretrained transformers exhibit the ability to predict unseen dynamical systems (Fig. 1A). These forecasts exceed the quality of naive baselines like mean regression, suggesting that transformers employ a more sophisticated in-context forecast strategy by leveraging their uniquely long context. During training on a single system (Train-ID), we see an early underfitting-to-overfitting transition on Test-ID, consistent with the classical bias-variance tradeoff: the model initially learns generalizable information about the system’s dynamics, leading to improvements on both seen and unseen data (Fig. 1B, gray and blue curves). However, as the Train-ID loss continues to fall, the model begins to overfit, leading to an increase in Test-ID error. At even later stages of training, we observe epoch-wise double descent, a recently-characterized phenomenon in which the Test-ID error further falls again below the classical bias-variance optimum [17–19]. However, we discover a *second*, earlier double descent curve in the Test-OOD error (Fig. 1B, magenta curve). This finding implies that information generalizable to other dynamical systems becomes available to the transformer during the pretraining process, but that it is bounded from above by ID-system-specific information.

Where does this generalization signal come from? We sample the transformer’s time-delayed conditional distribution $\hat{p}(x_{t+1}|x_{t-k})$, $k \leq C$ averaged across Test-OOD for all lag values $k \in 0, 1, \dots, C$. We find that this distribution qualitatively resembles the true attractor of Test-OOD, implying that the univariate model identifies relevant information about the unobserved multivariate attractor during testing (Fig. 2A). This result is consistent with Takens’ theorem: a univariate time series arising from an attractor with intrinsic dimension $d_{\mathcal{M}}$ can be embedded using $d_E = 2d_{\mathcal{M}} + 1$ time delays. We thus refer to the time delay coordinates $\hat{\mathbf{y}}_i = [\mathbf{x}_{i-d_E}, \dots, \mathbf{x}_i]$ as an estimate of the unobserved true phase space coordinates \mathbf{y} [20, 21].

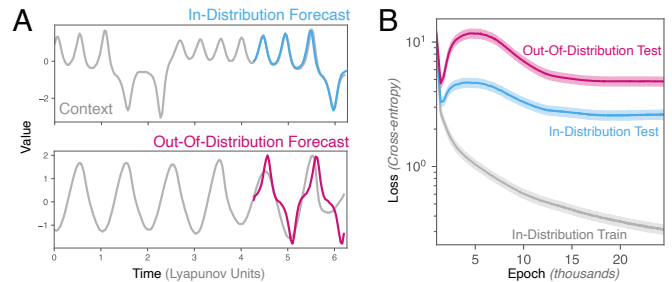


Figure 1. **Double descent during in-context learning of dynamical systems.** (A) Forecasts from a transformer trained on univariate time series from one dynamical system (Train-ID) then evaluated on its ability to forecast unseen trajectories from the same system (Test-ID, blue), versus forecasts of trajectories from an unseen system (Test-OOD, magenta). Gray curve shows the context, a subset of the total training data. (B) Loss curves on the training data, versus held-out in-distribution and out-of-distribution validation sets. Ranges are standard errors across 100 replicate experiments, each corresponding to a different randomly-sampled train/test pair of dynamical systems.

To test the scaling predicted by Takens’ theorem, we generate new Test-OOD trajectories using the Lorenz-96 system, a dynamical system with a controllable number of dynamical variables D [22]. This system’s manifold dimension $d_{\mathcal{M}}$ scales approximately linearly with D (Appendix D). As we vary the number of dynamical variables in Test-OOD $D = 3, 4, \dots, 25$, we evaluate the average Test-OOD accuracy of transformers originally trained on a different dynamical system (Train-ID) with $D = 3$. For each test case, we compare the transformer’s empirical order- k conditional distribution (averaged across Test-OOD) to a k -order Markov chain $p(x_{t+1}|x_t, x_{t-1}, \dots, x_{t-k-1})$ trained directly on Test-OOD, in order to estimate the effective order k of the Markov chain best-approximating the transformer’s Test-OOD dynamics. We find that the order of the best-approximating Markov chain scales with the intrinsic dimension of Test-OOD (Fig. 2C). This finding is striking, because the univariate Test-OOD series contains no direct information about the true dimensionality D or $d_{\mathcal{M}}$, suggesting that the transformer instead leverages information from time delay embedding in-context.

To confirm that this effect arises from the transformer’s internal representations, for each Test-OOD example, we calculate the attention rollout matrix $A_{\text{roll}} \in \mathbb{R}^{C \times C}$ [23]. This metric measures the sparsity of the model’s attention to different token positions, averaged across the entire testing set and both attention heads. We compute the stable rank of the rollout matrix ($d_{\text{latent}} = \text{srank}(A_{\text{roll}})$) as a measure of the intrinsic dimensionality of the transformer’s latent representations. We find that increasing attractor dimension $d_{\mathcal{M}}$ strongly correlates with increasing latent dimensionality d_{latent} . Because the univariate time series presented to the transformer lack direct information about dimensionality, we

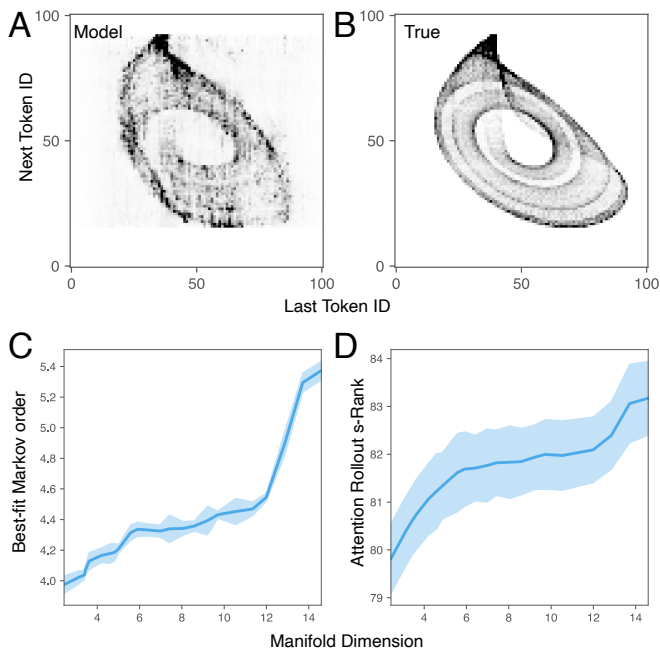


Figure 2. **Transformers perform time-delay embedding during inference.** (A) Empirical time-delayed next-token probabilities $p_{\text{model}}(x_{t+1}|x_{t-k})$ averaged across Test-OOD context for a transformer trained on a different system (Train-ID). (B) Exact next-token probabilities $p_{\text{true}}(x_{t+1}|x_{t-k})$ obtained from fitting a Markov chain on a long sample of Test-OOD. (C) The order of the closest-approximating Markov chain, versus the true intrinsic dimension $d_{\mathcal{M}}$ of the full attractor from which the univariate Test-OOD trajectory originates. (D) The effective dimension (stable rank) of the transformer’s attention rollout matrix versus the true intrinsic dimension of Test-OOD. Each point is an average over 100 replicate models trained on a different low-dimensional dynamical system.

conclude that the trained model infers information about the underlying attractor via in-context learning. Thus, not only does the transformer embed the test time series, it does so adaptively by identifying when a univariate time series arises from a high-dimensional system.

We next consider how the model pushes forward the dynamics on the dynamical coordinates $\hat{\mathbf{y}}$. Broadly, there are two ways that a surrogate model could represent a dynamical propagator, given finite-length context: (1) a differential form based on approximating time derivatives (as in multi-step integrators, or differential equation inference methods like SINDy), or (2) an integral approach that approximates a transfer operator (as in neural operators or discrete-time system identification) [24, 25]. Based on the coincidence of the trained model’s empirical logit distribution with a Markov chain, we hypothesize the latter: transformers approximate propagators in-context.

To test this hypothesis, we extract the empirical transition matrix of the transformer on the space of length- k delay vectors $\hat{\mathbf{y}}_t$ by aggregating multi-step predictions

from the model $\hat{p}(x_{t+1} | \mathbf{x}_C)$. Briefly, across Test-OOD we tabulate each distinct k -gram (\mathbf{x}_k , $k < C$), and we group together all context sequences \mathbf{x}_C that end in that k -gram. For each unique k -gram, we randomly-sample from all matching context sequences and predict the frequency of the next token x_{t+1} . By repeating this process separately for each k -gram, we can estimate a transfer operator on the time-delayed sequence $p(\hat{\mathbf{y}}_{t+1} | \hat{\mathbf{y}}_t) \equiv p(x_{t+1}, x_t, \dots, x_{t-k} | x_t, x_{t-1}, \dots, x_{t-k-1})$. This row-stochastic transition matrix describes the model-implied dynamics on the lag- k state space embedding of the univariate Test-OOD time series.

We compare the empirical operator to the ground truth operator $p(\mathbf{y}_{t+1} | \mathbf{y}_t)$, which we estimate from the *fully-observed* state space using Ulam’s method, which discretizes the full multivariate phase space and tabulates all transition rates between pairs of regions [26]. We observe that the leading eigenvalues (ranked by $|\lambda_i|$) closely match, implying that the transformer captures the dominant timescales associated with the Perron-Frobenius operator propagating the dynamics (Fig. 3B). The corresponding eigenfunctions represent the stationary distribution $\pi^{(0)}$ and subleading eigenfunctions $\pi^{(1)}$, $\pi^{(2)}$ corresponding to long-lived metastable trapping regions, known as *almost-invariant sets* [27]. These eigenfunctions occur in pairs due to symmetry (Fig. 3A).

To confirm that the onset of OOD generalization during training arises from test-time inference of the underlying propagator, we directly compare the Test-OOD loss to the KL divergence $D_{KL}(\pi^{(0)} || \hat{\pi}^{(0)})$ between the true and model-implied invariant distributions. Across hundreds of unique pairs of systems, we observe consistent correlation between Test-OOD loss and distributional distance (Fig. 3C). We thus conclude that, as the transformer’s out-of-distribution performance improves, it learns in-context an increasingly accurate estimate of the Perron-Frobenius operator of the fully-observed true system.

Taken together, our results show that, during inference, transformers trained on dynamical systems first learn to perform time delay embedding on the context, and then use co-occurrence statistics to approximate the true transfer operator of the fully-observed state space. Our work thus provides an example of how a learning model can extract a system-independent forecasting strategy despite system-specific training, beyond naive strategies observed in prior works such as parroting sequences from the context [28]. Our work thus provides a potential explanation for recent works showing the surprising ability of pretrained foundation models to forecast dynamical systems outside their training data, such as turbulent flows, weather fronts, or plasma dynamics [2, 11, 29]. Additionally, our observation of in-context time delay embedding supports findings throughout the broader time series literature, that univariate models often match the performance of multivariate models, even for datasets with strong covariates [30]. It also accords with a recent theoretical result showing that single-layer

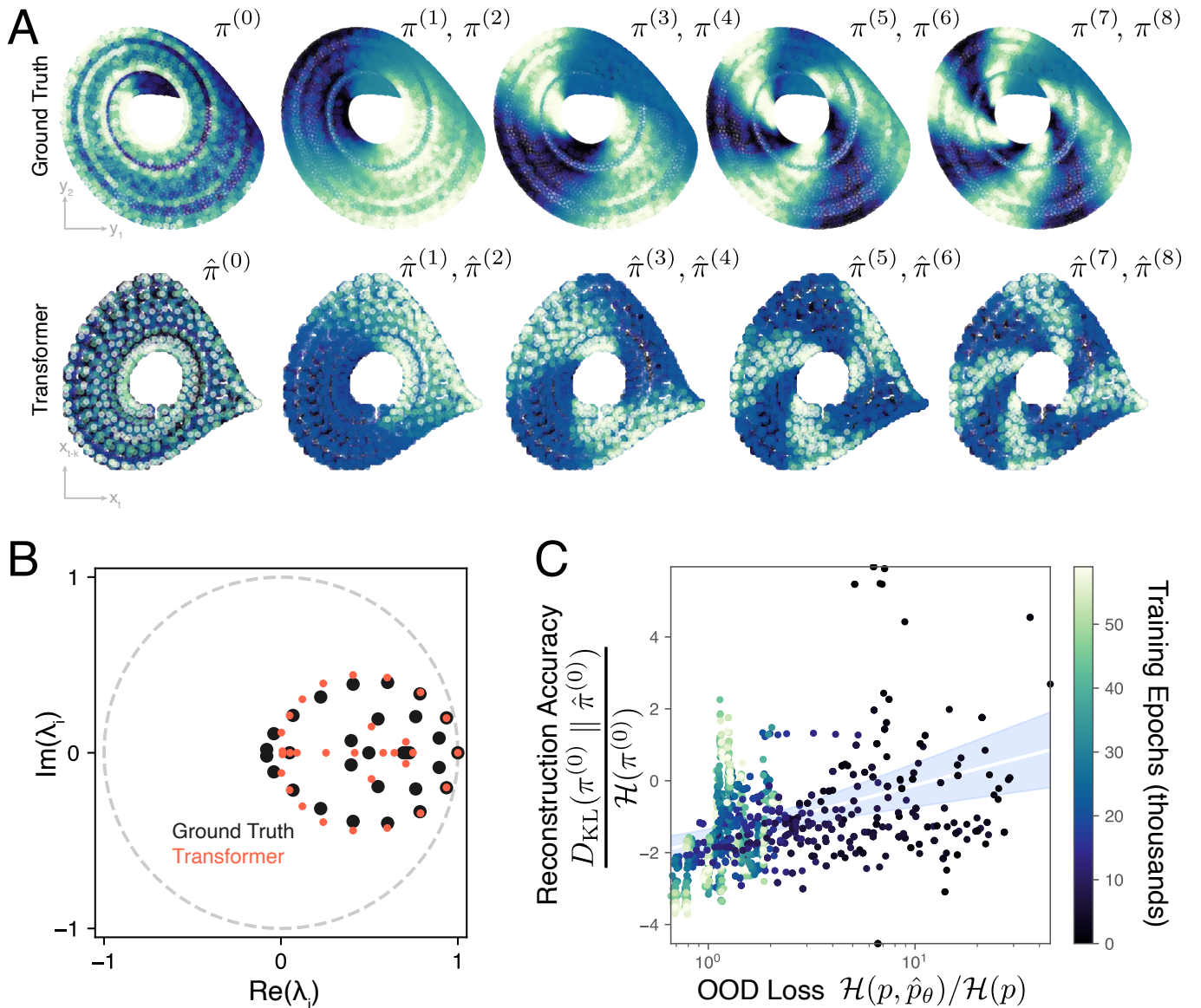


Figure 3. **Transformers learn in-context transfer operators on reconstructed dynamical manifolds.** (A) (Top) The true invariant distribution ($\pi^{(0)}(\mathbf{y})$) and longest-lived metastable distributions ($\pi^{(i)}(\mathbf{y})$ $i > 0$, almost-invariant sets) estimated from the fully-observed state space as the leading eigenvectors of the fully-observed transfer operator $p(\mathbf{y}_{t+1}|\mathbf{y}_t)$ (ranked by $|\lambda_i|$). (Bottom) The invariant and metastable distributions of the transformer, based on its next-token prediction probabilities over time-delayed univariate Test-OOD input sequences. Distributions are estimated as the leading eigenvectors of the lag- K conditional probabilities $\hat{p}(x_{t+1}\dots x_{t-K+2}|x_t\dots x_{t-K+1})$ derived from the transformer probabilities. Because the transformer is univariate, eigenvectors are plotted on the time-delay embedding $\hat{\mathbf{y}} \equiv [x_t, \dots, x_{t-K}]$. (B) The eigenvalue spectrum of the transfer operator estimated from the fully-observed attractor, and the implicit transfer operator of the transformer. (C) The KL divergence between the ground-truth invariant distribution of the transfer operator, and transformer empirical operator’s distribution, versus both Test-OOD validation loss and training epoch (color). A 95% confidence interval linear fit is underlaid (blue).

transformers can implement adaptive time-delay embedding in-context, given sufficient latent dimensionality [31]. Finally, our results support recent neural scaling laws showing improved performance of time series and scientific foundation models with additional context [32].

Reminiscent of similar findings in language models [33], our work demonstrates how the unique quadratic complexity of attention-based models enables the emergence of nontrivial strategies for estimating and propagating dynamical states.

- [1] S. Subramanian, P. Harrington, K. Keutzer, W. Bhimji, D. Morozov, M. W. Mahoney, and A. Gholami, Towards foundation models for scientific machine learning: Characterizing scaling and transfer behavior, *Advances in Neural Information Processing Systems* **36**, 71242 (2023).
- [2] M. McCabe, B. Régaldou-Saint Blancard, L. Parker, R. Ohana, M. Cranmer, A. Bietti, M. Eickenberg, S. Golkar, G. Krawezik, F. Lanusse, *et al.*, Multiple physics pretraining for spatiotemporal surrogate models, *Advances in Neural Information Processing Systems* **37**, 119301 (2024).
- [3] M. A. Rahman, R. J. George, M. Elleithy, D. Leibovici, Z. Li, B. Bonev, C. White, J. Berner, R. A. Yeh, J. Kossai, *et al.*, Pretraining codomain attention neural operators for solving multiphysics pdes, *Advances in Neural Information Processing Systems* **37**, 104035 (2024).
- [4] M. Herde, B. Raonic, T. Rohner, R. Käppli, R. Molinaro, E. De Bezenac, and S. Mishra, Poseidon: Efficient foundation models for pdes, *Advances in Neural Information Processing Systems* **37**, 72525 (2024).
- [5] M. McCabe, P. Mukhopadhyay, T. Marwah, B. R.-S. Blancard, F. Rozet, C. Diaconu, L. Meyer, K. W. Wong, H. Sotoudeh, A. Bietti, *et al.*, Walrus: A cross-domain foundation model for continuum dynamics, *arXiv preprint arXiv:2511.15684* (2025).
- [6] T. Brown, B. Mann, N. Ryder, M. Subbiah, J. D. Kaplan, P. Dhariwal, A. Neelakantan, P. Shyam, G. Sastry, A. Askell, *et al.*, Language models are few-shot learners, *Advances in neural information processing systems* **33**, 1877 (2020).
- [7] J. Von Oswald, E. Niklasson, E. Randazzo, J. Sacramento, A. Mordvintsev, A. Zhmoginov, and M. Vladymyrov, Transformers learn in-context by gradient descent, in *International Conference on Machine Learning* (PMLR, 2023) pp. 35151–35174.
- [8] E. Akyürek, D. Schuurmans, J. Andreas, T. Ma, and D. Zhou, What learning algorithm is in-context learning? investigations with linear models, in *The Eleventh International Conference on Learning Representations* (2023).
- [9] N. A. Göring, F. Hess, M. Brenner, Z. Monfared, and D. Durstewitz, Out-of-domain generalization in dynamical systems reconstruction, in *Proceedings of the 41st International Conference on Machine Learning*, Proceedings of Machine Learning Research, Vol. 235, edited by R. Salakhutdinov, Z. Kolter, K. Heller, A. Weller, N. Oliver, J. Scarlett, and F. Berkenkamp (PMLR, 2024) pp. 16071–16114.
- [10] B. Clavier, D. Zarzoso, D. Del-Castillo-Negrete, and E. Frénod, Generative-machine-learning surrogate model of plasma turbulence, *Physical Review E* **111**, L013202 (2025).
- [11] S. G. Rosofsky and E. A. Huerta, Magneto-hydrodynamics with physics informed neural operators, *Machine Learning: Science and Technology* **4**, 035002 (2023).
- [12] S. Garg, D. Tsipras, P. S. Liang, and G. Valiant, What can transformers learn in-context? a case study of simple function classes, *Advances in neural information processing systems* **35**, 30583 (2022).
- [13] G. Reddy, The mechanistic basis of data dependence and abrupt learning in an in-context classification task, in *The Twelfth International Conference on Learning Representations* (2024).
- [14] E. Edelman, N. Tsilivis, B. Edelman, E. Malach, and S. Goel, The evolution of statistical induction heads: In-context learning markov chains, *Advances in Neural Information Processing Systems* **37**, 64273 (2024).
- [15] A. F. Ansari, L. Stella, C. Turkmen, X. Zhang, P. Mer- cado, H. Shen, O. Shchur, S. S. Rangapuram, S. P. Arango, S. Kapoor, *et al.*, Chronos: Learning the language of time series, *Transactions on Machine Learning Research* (2024).
- [16] W. Gilpin, Chaos as an interpretable benchmark for forecasting and data-driven modelling, *NeurIPS* **34** (2021).
- [17] M. Belkin, D. Hsu, S. Ma, and S. Mandal, Reconciling modern machine-learning practice and the classical bias-variance trade-off, *Proceedings of the National Academy of Sciences* **116**, 15849 (2019).
- [18] J. W. Rocks and P. Mehta, Memorizing without overfitting: Bias, variance, and interpolation in overparameterized models, *Physical review research* **4**, 013201 (2022).
- [19] P. Nakkiran, G. Kaplun, Y. Bansal, T. Yang, B. Barak, and I. Sutskever, Deep double descent: Where bigger models and more data hurt, *Journal of Statistical Mechanics: Theory and Experiment* **2021**, 124003 (2021).
- [20] F. Takens, Dynamical systems and turbulence, *Warwick*, 1980, 366 (1981).
- [21] J. Botvinick-Greenhouse, R. Martin, and Y. Yang, Invariant measures in time-delay coordinates for unique dynamical system identification, *Physical Review Letters* **135**, 167202 (2025).
- [22] E. N. Lorenz, Predictability: A problem partly solved, in *Proc. Seminar on predictability*, Vol. 1 (Reading, 1996) pp. 1–18.
- [23] S. Abnar and W. Zuidema, Quantifying attention flow in transformers, in *Proceedings of the 58th annual meeting of the association for computational linguistics* (2020) pp. 4190–4197.
- [24] J. Buzhardt, C. R. Constante-Amores, and M. D. Graham, On the relationship between koopman operator approximations and neural ordinary differential equations for data-driven time-evolution predictions, *Chaos: An Interdisciplinary Journal of Nonlinear Science* **35** (2025).
- [25] S. L. Brunton and J. N. Kutz, *Data-driven science and engineering: Machine learning, dynamical systems, and control* (Cambridge University Press, 2022).
- [26] S. M. Ulam, *A Collection of Mathematical Problems* (Interscience Publishers, New York, 1960) p. 150.
- [27] G. Froyland and M. Dellnitz, Detecting and locating near-optimal almost-invariant sets and cycles, *SIAM Journal on Scientific Computing* **24**, 1839 (2003).
- [28] Y. Zhang and W. Gilpin, Context parroting: A simple but tough-to-beat baseline for foundation models in scientific machine learning, in *The Fourteenth International Conference on Learning Representations* (2026).
- [29] I. Price, A. Sanchez-Gonzalez, F. Alet, T. R. Anderson, A. El-Kadi, D. Masters, T. Ewalds, J. Stott, S. Mohamed, P. Battaglia, *et al.*, Probabilistic weather forecasting with machine learning, *Nature* **637**, 84 (2025).
- [30] Y. Nie, N. H. Nguyen, P. Sinthong, and J. Kalagnanam, A time series is worth 64 words: Long-term forecasting with transformers, in *The Eleventh International Conference on Learning Representations* (2023).
- [31] G. Duthé, N. Evangelou, W. Liu, I. G. Kevrekidis, and E. Chatzi, A mechanistic analysis of transformers for dynamical systems, *arXiv preprint arXiv:2512.21113* (2025).
- [32] J. Lai, A. Bao, and W. Gilpin, Panda: A pretrained forecast model for universal representation of chaotic dynamics, in *The Fourteenth International Conference on Learning Representations* (2026).
- [33] R. Zhang, S. Frei, and P. L. Bartlett, Trained transformers learn linear models in-context, *Journal of Machine Learning Research* **25**, 1 (2024).
- [34] C. Raffel, N. Shazeer, A. Roberts, K. Lee, S. Narang,

- M. Matena, Y. Zhou, W. Li, and P. J. Liu, Exploring the limits of transfer learning with a unified text-to-text transformer, *Journal of machine learning research* **21**, 1 (2020).
- [35] A. Vaswani, N. Shazeer, N. Parmar, J. Uszkoreit, L. Jones, A. N. Gomez, L. Kaiser, and I. Polosukhin, Attention is all you need, *Advances in neural information processing systems* **30** (2017).
- [36] J. L. Ba, J. R. Kiros, and G. E. Hinton, Layer normalization, *arXiv preprint arXiv:1607.06450* (2016).
- [37] I. Loshchilov and F. Hutter, Decoupled weight decay regularization, *arXiv preprint arXiv:1711.05101* (2017).
- [38] P. Grassberger and I. Procaccia, Measuring the strangeness of strange attractors, *Physica D: nonlinear phenomena* **9**, 189 (1983).
- [39] A. Clauset, C. R. Shalizi, and M. E. Newman, Power-law distributions in empirical data, *SIAM review* **51**, 661 (2009).

APPENDIX

CONTENTS

References	5
Appendix	7
Appendix	7
Appendix A. Code Availability	7
Appendix B. Model architecture and training	7
A. Architecture	7
B. Tokenization	7
C. Training	8
D. Inference	8
Appendix C. Estimating the fully-observed transfer operator with Ulam’s method	8
Appendix D. Estimating the manifold dimension of the Lorenz-96 system	9
Appendix E. Attention rollout	9

Appendix A. CODE AVAILABILITY

The code used in this study is available at <https://github.com/williamgilpin/icicl>

Appendix B. MODEL ARCHITECTURE AND TRAINING**A. Architecture**

We implement a compact causal language model operating on a discrete vocabulary ($V = 100$) that predicts the next token autoregressively. Our model is a decoder-only transformer, similar to GPT models but with relative positional embedding akin to the T5 family [6, 34]. Each input token is mapped to a higher-dimensional embedding ($d_{\text{model}} = 256$). The network itself consists of two identical Transformer-style residual blocks, each using single-head causal self-attention, with query and key projections into $d_k = 128$ dimensions, and a value projection back into d_{model} [35]. Attention logits are scaled by $d_k^{-1/2}$ and strictly masked with a lower-triangular causal mask. Each block applies pre-normalization with LayerNorm before attention [36], then adds the attention output residually, and then applies a second LayerNorm followed by a position-wise feed-forward network with expansion factor 2 (resulting in hidden width $2d_{\text{model}} = 512$), using ReLU activation and a second linear layer returning to d_{model} , again added residually. A final LayerNorm precedes the output projection to logits over the vocabulary. The output projection is weight-tied to the input embedding matrix. The maximum context length is a fixed block size of $T_{\text{max}} = 512$ tokens. Positional information is encoded using ALiBi, an additive attention-logit bias proportional to the nonnegative lag distance with slope $\alpha = 1.0$, i.e. a term $-\alpha(i - j)$ for $i \geq j$ and 0 otherwise.

B. Tokenization

We convert real-valued time series into tokens with mean scaling followed by uniform scalar quantization into V bins, following the approach used in the first generation of the Chronos family of time series foundation models [15]. We favor direct quantization over patch-based approaches used in other time series foundation models due to the interpretability of the token space, and because it allows us to design our study based on prior studies of in-context generalization in language models [12].

Given training time series $x_{1:T}$ of length T , we compute a scale factor from the context

$$s = \max\left(\frac{1}{T} \sum_{i=1}^T |x_i|, \varepsilon\right), \quad \varepsilon = 10^{-8},$$

and we then normalize the entire series $\tilde{x}_i = x_i/s$. The normalized values are discretized into integer bin IDs in $\{1, \dots, V\}$ using uniformly spaced bin centers c_j spanning $[c_{\min}, c_{\max}]$ (with c_{\min} and c_{\max} treated as hyperparameters), and decision boundaries placed at midpoints between adjacent centers, with outer edges extending to $\pm\infty$ so that all values map to a unique bin. A reserved “padding” token uses ID 0. Missing values (NaNs) are handled by replacing their contribution with 0 for purposes of scale computation, while their token positions are set to the padding ID 0 in the emitted token sequence. Decoding maps bin IDs back to their corresponding centers and rescales via $\hat{x}_i = s \tilde{x}_i$.

C. Training

We train our model using next-token prediction with cross-entropy loss over the vocabulary. We quantize the training time series and provide it to the model as a single long one-dimensional token stream, from which we sample fixed-length windows of length $T = 512$ uniformly at random: the input is a contiguous block of 512 tokens and the target is the same block shifted by one position. The effective dataset length is treated as a large virtual size (10,000 samples) with random window sampling each time. We optimize the model using AdamW with learning rate 5×10^{-5} , weight decay 0.0, batch size 32, with gradient accumulation over micro-batches (with default size 1) by averaging loss across micro-steps before backpropagation [37]. We clip gradients to a maximum global norm of 1.0 at each step. We train for 50,000 optimization steps and perform validation every 1000 steps by evaluating cross-entropy on one randomly sampled validation batch, and additionally on a separate out-of-distribution validation stream of the same form. We do not use a learning-rate schedule.

D. Inference

We perform autoregressive inference for a specified number of new tokens H beyond the provided context. At each step, we use only the most recent $C = 512$ context tokens. The model outputs logits for the next token, which are converted to a token choice either greedily (argmax, temperature 0) or by sampling. We append the sampled token to the context, and repeat the process for H steps, yielding a lengthened token sequence. If a real-valued time series is needed for downstream analysis, we decode the output token sequence back to real values via dequantization to bin centers followed by multiplication by the stored mean scale s .

Appendix C. ESTIMATING THE FULLY-OBSERVED TRANSFER OPERATOR WITH ULAM’S METHOD

Let $\{\mathbf{y}_t\}_{t=0}^{N-1}$ be a time series (discrete-time) sampled at uniform intervals τ from a trajectory $\mathbf{y}(t) \in \mathbb{R}^D$ in the fully-observed phase space. We construct a finite-rank approximation of the Perron-Frobenius (transfer) operator at lag $\tau > 0$ by (1) partitioning the D -dimensional phase space into K bins, (2) symbolizing the trajectory by bin labels, and (3) estimating the induced Markov transition matrix between bins.

Partition and symbolic dynamics. We partition $\{B_1, \dots, B_K\}$ the data $\{\mathbf{y}_t\}$ by clustering. Given a set of samples $\{\mathbf{y}_t\}$ we use K -means clustering to generate Voronoi cells $B_i \equiv \{\mathbf{y} : \arg \min_j \|\mathbf{y} - \mathbf{c}_j\| = i\}$ with centers $\{\mathbf{c}_i\}_{i=1}^K$, $\mathbf{c}_i \in \mathbb{R}^D$. This defines a (hard) coding map $\kappa : \mathbf{y} \rightarrow \{1, \dots, K\}$, which we apply to the training data to generate the symbolic sequence

$$s_t := \kappa(\mathbf{y}_t) \in \{1, \dots, K\}.$$

Empirical Ulam matrix at lag τ . For a fixed lag τ , Ulam’s method approximates the transfer operator \mathcal{P}_τ by the $K \times K$ matrix $P^{(\tau)}$ as

$$P_{ij}^{(\tau)} \approx \mathbb{P}(s_{t+\tau} = j \mid s_t = i),$$

i.e., the probability mass transferred from bin B_i to bin B_j over time τ . We compute this quantity by counting all transition pairs, and dividing by the total number of transitions.

Estimating the transfer operator spectrum. Once $P^{(\tau)} \in \mathbb{R}^{K \times K}$ is obtained, we treat it as a Markov operator. We estimate the stationary distribution $\pi^{(0)}$ from the invariant left eigenvector of $P^{(\tau)}$,

$$\pi^\top P^{(\tau)} = \pi^\top, \quad \sum_{i=1}^K \pi_i = 1, \quad \pi_i \geq 0.$$

We solve this using power iteration on $(P^{(\tau)})^\top$.

We estimate long-lived transient modes $\pi^{(i)}$, $i > 0$ by applying power iteration to a deflated operator that removes the stationary mode. Writing $\mathbf{1}$ for the all-ones vector, the deflation

$$\tilde{P}^{(\tau)} = P^{(\tau)} - \mathbf{1} \pi^\top$$

annihilates the stationary left eigenvector and allows us to estimate the leading subdominant left modes (metastable transients) with power iteration.

Choice of partition size. Because Ulam discretization trades bias (too few bins) against variance/sparsity (too many bins), we scan over candidate K and select a value that yields informative, non-degenerate transition structure. We compute a row-wise entropy statistic of $P^{(\tau)}$ across K and choose values that maximize this statistic. This heuristic favors partitions that are neither so large that most transitions are self-loops, nor so small that the transition matrix becomes overly sparse.

Appendix D. ESTIMATING THE MANIFOLD DIMENSION OF THE LORENZ-96 SYSTEM

We consider the D -dimensional Lorenz-96 system with constant forcing,

$$\dot{X}_i = (X_{i+1} - X_{i-2})X_{i-1} - X_i + F, \quad i = 1, \dots, D, \quad (\text{A1})$$

with cyclic boundary conditions $X_{i+n} = X_i$ and $X_{i-n} = X_i$. Here $X_i(t)$ are the state variables, D is the system dimension, and F is the constant external forcing. In all simulations we set $F = 8.0$. The initial condition is taken as $X_i(0) = F$ for all i , with a random normal perturbation of 10^{-2} added to the first component to ensure diversity across generated trajectories. The system is integrated to 1000 time units using the implicit Radau IIA method. We discard the first 500 steps of the generated trajectory as transients.

Given a multivariate time series $\{\mathbf{y}_i\}_{i=1}^N \subset \mathbb{R}^D$, the Grassberger-Procaccia calculation is implemented by first forming the full matrix of pairwise Euclidean distances $\rho_{ij} = \|\mathbf{y}_i - \mathbf{y}_j\|_2$ and collecting all strictly positive distances into a single sample $\{\rho_k\}_{k=1}^K$ [38]. To focus on the intermediate scaling regime and reduce the influence of (1) discretization effects at very small separations and (2) finite-size saturation at large separations, the distance sample is truncated by discarding values below the 5th percentile and above the 50th percentile. The remaining distances are treated as draws from a power-law tail $p(\rho) \propto \rho^{-\alpha}$ for $\rho \geq \rho_{\min}$, where ρ_{\min} is taken as the minimum retained distance, and the exponent is estimated by the continuous maximum-likelihood formula $\hat{\alpha} = 1 + \left[\frac{1}{K} \sum_{k=1}^K \ln(\rho_k / \rho_{\min}) \right]^{-1}$ [39]. This scaling exponent is interpreted as the manifold dimension $d_{\mathcal{M}}$.

To measure the scaling of the manifold dimension $d_{\mathcal{M}}$ with the dynamical dimension D , we generate trajectories from the Lorenz-96 system with varying number of dynamical variables $D = 5, 6, 7, \dots, 25$, and perform the Grassberger-Procaccia algorithm separately for each trajectory (Fig. S1). We observe a linear scaling of the manifold dimension $d_{\mathcal{M}}$ with the dynamical dimension D .

Appendix E. ATTENTION ROLLOUT

For a fixed context length C and an input token sequence $\mathbf{x}_C \in \mathbb{Z}^C$, let $A^{(\ell)}(\mathbf{x}_C) \in \mathbb{R}^{C \times C}$ denote the causal self-attention matrix produced by layer $\ell \in \{1, \dots, L\}$ (though we set $L = 2$ in our experiments), where each row is a probability distribution over past positions (row-stochastic under the softmax and causal mask). Following [23], we incorporate residual mixing by defining the augmented layer-wise transition

$$\tilde{A}^{(\ell)}(\mathbf{x}_C) = I + A^{(\ell)}(\mathbf{x}_C), \quad (\text{A2})$$

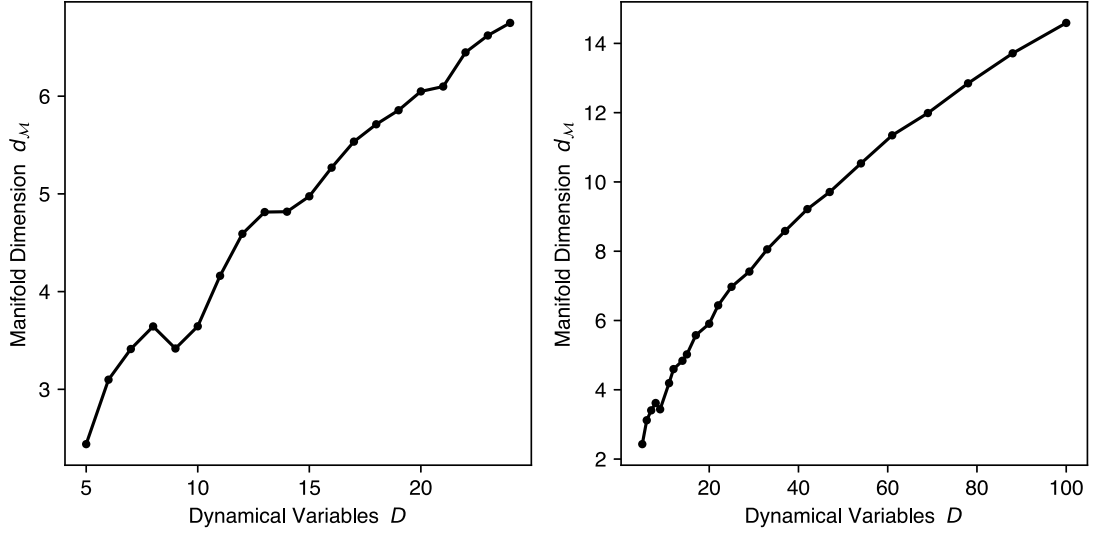


Figure S1. The estimated manifold dimension $d_{\mathcal{M}}$ of the attractor of the Lorenz-96 system as the number of dynamical variables D varies.

and propagate attention through depth by matrix multiplication,

$$A_{\text{roll}}(\mathbf{x}_C) = \tilde{A}^{(L)}(\mathbf{x}_C) \tilde{A}^{(L-1)}(\mathbf{x}_C) \cdots \tilde{A}^{(1)}(\mathbf{x}_C) \in \mathbb{R}^{C \times C}. \quad (\text{A3})$$

The entry $(A_{\text{roll}})_{ij}$ can be interpreted as the effective contribution (via all compositional attention paths across layers) of token position j to the representation at position i . In practice, we average $A_{\text{roll}}(\mathbf{x}_C)$ across the Test-OOD contexts to obtain a single rollout matrix $A_{\text{roll}} \in \mathbb{R}^{C \times C}$ summarizing how the trained model distributes influence across lags; we then quantify its effective dimensionality using the stable rank $d_{\text{latent}} = \text{srank}(A_{\text{roll}}) = \|A_{\text{roll}}\|_F^2 / \|A_{\text{roll}}\|_2^2$.